Soft Matter

Accepted Manuscript

ROYAL SOCIETY OF CHEMISTRY

www.rsc.org/softmatter

ARTICLE TYPE www. rsc.org/xxxxxx | XXXXXXXX

Structural relaxation in glassy polymers predicted by soft modes: A quantitative analysis

Anton Smessaert[*a] **and Jörg Rottler**[a]

Received Xth XXXXXXXXXX 20XX, Accepted Xth XXXXXXXXX 20XX
First published on the web Xth XXXXXXXXXX 200X
DOI: 10.1039/b000000x

We present a quantitative analysis of the correlation between quasi-localized, low energy vibrational modes and structural relaxation events in computer simulations of a quiescent, thermal polymer glass. Our results extend previous studies on glass forming binary mixtures in 2D, and show that the soft modes identify regions that undergo irreversible rearrangements with up to 7 times the average probability. We study systems in the supercooled- and aging-regimes and discuss temperature- as well as age-dependence of the correlation. In addition to the location of rearrangements, we find that soft modes also predict their *direction* on the molecular level. The soft regions are long lived structural features, and the observed correlations vanish only after $> 50\%$ of the system has undergone rearrangements.

1 Introduction

When a polymer melt is cooled to close to the glass transition temperature, the dynamics on the molecular scale becomes increasingly *heterogeneous*[1]. Transient regions of low and high mobility emerge and plastic events are concentrated in the more mobile parts. The resulting dynamical heterogeneity (DH) lies at the heart of current understanding of the glass transition, but it is furthermore a universal feature of the larger class of amorphous solids. Computer simulations strongly suggest that there exists at least a partial link between DH and the molecular structure[2,3]. However, a clear understanding of the structural features that are responsible for making a region "soft" and therefore prone to rearrangements is still missing. This lack of insight stands in the way of an atomistic theory of plasticity for glassy polymers and more generally for amorphous solids that is akin to the dislocation-centered theories for crystal plasticity.

A crucial step in understanding the link between dynamics and structure is the identification of structurally "soft" regions without dynamical information. Recently, a lot of interest has focused on the low energy vibrational modes as such an identifier. Already 20 years ago, it was observed that in glassy materials some low energy modes are "quasi-localized"[4–6] with only few particles effectively participating in a mode. This is caused by the scattering of phonons at the local structure surrounding these easily excitable particles. Recently, Widmer-Cooper et al.[7] revealed a qualitative correlation between the location of these quasi-localized, low energy modes or *soft modes* and irreversible molecular rearrangements. The correlation was observed in computer simulations of a binary mixture in 2D[7] and 3D[8] in the supercooled regime and it successfully linked DH to a structural property, the vibrational spectrum. Further indications for this link were found in simulations of hard spheres[9], a kinetically constrained lattice glass[10], a quasi-statically sheared binary glass in 2D[11], and experiments on colloidal glasses[12]. A striking quantitative correlation was verified by Manning and Liu[13], showing that local plastic rearrangements overlap with "soft spots". The study focused on a binary glass in 2D under quasi-static shear at zero temperature, and the soft spots were identified by accumulating the most participating particles in the lowest energy modes in a binary soft spot map. This correlation between soft spots and plastic events was recently found to hold also in thermal binary glasses at finite shear rate[14].

To fully understand the role of soft spots in plasticity of amorphous solids, it is important to test the robustness of the soft spot picture in other glass formers. In the present work, we quantitatively study the spatial correlation between soft modes and molecular rearrangements in a polymer glass model. To the best knowledge of the authors, this is the first quantitative study of a three-dimensional system, and it focuses on the case without external loading, the quiescent state. Systems above (supercooled regime) and below (aging regime) the glass transition temperature are analyzed, and we discuss the impact of temperature as well as aging on the correlation. The participation of particles in the soft modes is quantified following the superposition scheme proposed by Widmer-Cooper and coworkers[7,8,15]. The construction of this *softness field* requires fewer parameters than the related soft spot approach by Manning and Liu[13], because it avoids bi-

[a] *Department of Physics and Astronomy, University of British Columbia, 6224 Agricultural Road, Vancouver, B.C. V6T 1Z1, Canada*
E-mail: anton@physics.ubc.ca

narization. We present a comprehensive analysis of the lifetime of the softness field. We find it to be long lived compared to elementary vibrational timescales, therefore making it a meaningful structural variable. Rearrangements at soft regions occur with up to 7 times higher likelihood than on average. Moreover, we find the direction of segmental motion to be well correlated with the "soft directions" predicted by the vibrational spectrum.

Our findings are presented as follows: In section 2 we discuss the quasi-localized soft modes found in glassy materials and define a softness field in terms of a scalar value and direction as a measure of the heterogeneous structure in glasses. In section 3 we introduce the polymer model and glass creation protocol, and we explain simulation details, as well as the identification of relaxation events. The results are discussed in section 4. We first focus on the properties of the softness field, and in the following quantitatively analyze the spatial and directional correlation between structural relaxation events and the softness field. In the last section, the results are summarized and discussed.

2 Defining scalar and directional softness

The vibrational spectrum of amorphous solids exhibits a concentration of anomalous modes in the low energy range known as the boson peak[6,16–18]. Instead of extended plane-waves, the anomalous modes only involve a fraction of the system and are therefore "quasi-localized" in space. They are caused by the scattering of phonons at structurally distinct, disorder-features in the molecular structure. An example of such a quasi-localized mode is shown in Fig. 1a, where the activity is concentrated in three "soft spots". In computer simulations, one can directly access the vibrational spectrum by diagonalizing the Hessian

$$H_{(\mathbf{r}_i)_k(\mathbf{r}_j)_l} = \frac{\partial^2 U(\{\mathbf{r}_i\})}{\partial(\mathbf{r}_i)_k \partial(\mathbf{r}_l)_n} \,.$$

Here $U(\{\mathbf{r}_i\})$ is the potential energy and $(\mathbf{r}_i)_k$ is the k'th component of the position of particle i. The projection of eigenvector j of $\mathbf{H}$ on the degrees of freedom of particle i is the polarization vector $\mathbf{e}_j^{(i)}$, and one can calculate the extent of localization of mode j via its participation ratio

$$P_j = \frac{\left(\sum_{i=1}^{N} (\mathbf{e}_j^{(i)})^2\right)^2}{N \sum_{i=1}^{N} (\mathbf{e}_j^{(i)})^4} \,.$$

A value of $P_j = 1$ means that all particles are participating equally in mode j, whereas a small value indicates that the mode is quasi-localized around a few active particles. Figure 1b shows the density of states of the vibrational spectrum of our polymer glasses at different parameters, rescaled such that the boson peak is exposed. Similar distributions have been found in other amorphous solids[16,17]. The participation ratio of the spectrum is shown in panel 1c. We find an increase of $P(\omega)$ with growing eigenfrequency towards a value around 0.45 and the "quasi-localized" modes are concentrated prior and at the boson peak.

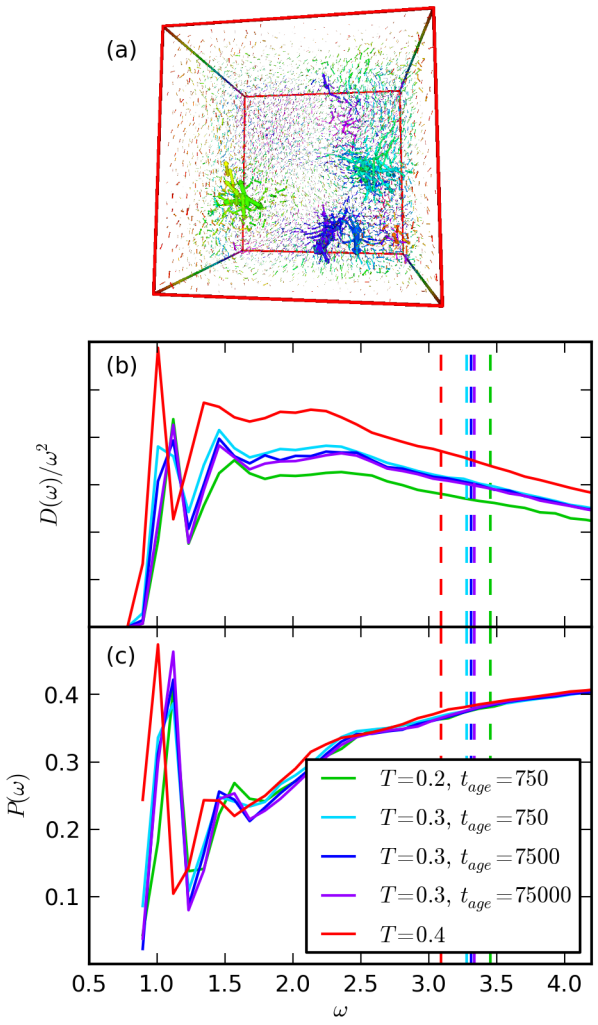

Fig. 1 (a) Exemplary soft mode with $\omega = 1.2$ and $P = 0.08$, visualized as polarization vector field. Coloring indicates depth. (b) Density of state of low energy vibrational modes, rescaled to reveal the boson peak. (c) Mean participation ratio as function of mode frequency. The color in (b,c) indicates the five studied systems (see section 3 for details) and each curve is an average over 20 realizations. The dashed lines indicate the cutoff $N_m = 600$ for each system.

Instead of attempting a binary decomposition into hard and soft regions[13], we characterize the softness of a particle by the

superposition of the participation fractions in the low energy vibrational modes[7,8,15],

$$\phi_i = \frac{1}{N_m} \sum_{j=1}^{N_m} |\mathbf{e}_j^{(i)}|^2 \,. \quad (1)$$

This softness field depends on a single parameter, the number of included low energy modes N_m, and the scaling factor is added to make the softness an intensive quantity in terms of N_m. A particle i is therefore considered "softer" the larger ϕ_i is. It is worth pointing out that the contribution of each mode should be weighted by its energy. A particle that is involved in a low energy mode requires less energy to be excited to the same extent than a particle with identical projection $|\mathbf{e}^{(i)}|^2$ in a higher frequency mode. However, we find that this weighting does not improve the predictive strength of the softness field for the present system, since the frequency does not vary strongly for the contributing modes. More details about the effect of this weighting as well as alternative definitions of softness are briefly discussed in the Appendix.

2.1 Direction of the modes

Directional information can be added to the scalar softness field in a similar superposition scheme. The eigenvector of mode j defines the direction for particle i via the projection vector $\mathbf{e}_j^{(i)}$. As mentioned above, this vector is defined up to its sign due to the harmonic nature of the description. In order to find the dominating direction in the N_m modes, we calculate nematic tensors from the unit length projection vectors $(Q_j^{(i)})_{\alpha,\beta} = \left(\frac{3}{2}\hat{e}_{j,\alpha}^{(i)}\hat{e}_{j,\beta}^{(i)} - \frac{1}{2}\delta_{\alpha,\beta}\right)$ and perform a weighted average

$$\mathbf{Q}_\phi^{(i)} = \frac{\sum_{j=1}^{N_m} \tilde{\phi}_j^{(i)} \mathbf{Q}_j^{(i)}}{\sum_{j=1}^{N_m} \tilde{\phi}_j^{(i)}} \,,$$

with weights $\tilde{\phi}_j^{(i)} = |\mathbf{e}_j^{(i)}|^2$ being the contribution of individual modes to the softness of particle i. The eigenvector of the largest eigenvalue of $\mathbf{Q}_\phi^{(i)}$ then defines the direction of the softness field $\mathbf{e}_\phi^{(i)}$.

3 Methods

The polymer glass is simulated using molecular dynamics techniques and the well-known finitely extensible nonlinear elastic (FENE) bead-spring model[19], which has excellent and well-documented glass-forming ability[20]. In this model a linear polymer consists of 50 identical beads that are linked into a chain via a non-linear stiff spring-like interaction that acts as covalent bonds and prevents chain-crossing. Inter- and intra-chain interactions between non-bonded beads are modeled with a 6-12 Lennard-Jones (LJ) potential. To improve computational efficiency the LJ potential is cut off at $r_c = 2.5\sigma$ and force-shifted[21] to ensure that a Hessian is defined. All results are given in the usual LJ units based on well energy ε, particle diameter σ, mass m and characteristic time scale $\tau_{LJ} = \sqrt{m\sigma^2/\varepsilon}$, which is just below twice the mean collision time. We simulate N=10,000 particles as 200 chains of 50 beads each in a simulation box with periodic boundary conditions in all dimensions. The system size was chosen relatively small due to computational constraints on the calculation of the vibrational modes (see below). The glass was generated following the protocol outlined in more detail in a previous study[22]: A melt is equilibrated and then rapidly quenched at constant quench rate and volume to the target temperature. The densities were chosen such that the pressure at the end of the quench is close to zero. A glass transition temperature of $T_g \simeq 0.4$ was estimated from the temperature dependence of the pressure during cooling. We investigated two glasses in the aging regime, at temperatures $T = 0.2, 0.3$, and one system at $T = 0.4$. At this latter temperature, the relaxation times are short enough so that the glass reached equilibrium shortly after the quench and is therefore a supercooled liquid. To evaluate aging effects, we analyzed the glass at $T = 0.3$ at three ages: $t_{age} = 7.5 \cdot 10^2, 7.5 \cdot 10^3, 7.5 \cdot 10^4$. All simulations at the final temperatures were performed in the quiescent state, at zero pressure in the NPT ensemble, using LAMMPS[23]. The results shown below are averaged over 20 realizations of each system with independent initial configurations, each run for $4 \cdot 10^8$ (10^7) time steps in the aging (supercooled) regime and with $\Delta t = 0.0075\tau_{LJ}$.

The two main measurements in our study are, on the one hand the softness field ϕ, and on the other hand the structural relaxation events. We identify the relaxation events using a detection algorithm that was introduced in a previous study[22] where it is explained in greater detail. In short, the crowded surroundings around each particle act as a cage, and the dynamics of the particle is reduced to vibrational motion while the local structure remains unchanged. Structural relaxation happens when a particle escapes its cage, resulting in rapid changes in the particle trajectory. We detect these *hops* on-the-fly during the simulation and record particle id, time of hop, as well as initial and final position. The algorithm works similar to a moving average and calculates the mean distance squared

$$P_{hop}^{(i)} = \sqrt{\left\langle \left(\mathbf{r}_i^A - \bar{r}_i^B\right)^2 \right\rangle_A \cdot \left\langle \left(\mathbf{r}_i^B - \bar{r}_i^A\right)^2 \right\rangle_B}$$

between the earlier (A) and later (B) half of the trajectory of particle i in a time window that moves with the simulation. Here, the averages $\langle . \rangle_A$ [$\langle . \rangle_B$] are taken over all trajectory points in A [B] and $\bar{r}^A$ [$\bar{r}^B$] is the mean position in the respective trajectory segment. A threshold criterion identifies the hops, which is linked to the plateau value of the mean

squared displacement. Here we use $P_{hop} = 0.15, 0.21, 0.27 = P_{th}$ as threshold values for the systems at temperature $T = 0.2, 0.3, 0.4$. In an additional evaluation step, we exclude back-and-forth hops of a particle between the same two positions. This is implemented by removing a sequence of two hops of the same particle, if the final position of the second hop is within a distance of $\sqrt{P_{th}}/2$ of the initial position of the first hop. With this adaptation, the hop detection algorithm gives a full map of the irreversible structural rearrangements on a molecular level.

The softness field at time t is measured from a snapshot of the system at that time, from which the inherent structure is identified using a combination of gradient descent and damped dynamics (FIRE[24]) algorithms with a minimal total force criterion. The Hessian is then calculated from the inherent structure and partially diagonalized using ARPACK[25]. The eigenmodes are then used to calculate the softness field as described above. An analysis of the maximal cross-correlation (see below) as a function of N_m (not shown) reveals a broad and weak maximum between $300 > N_m > 900$ (1-3% of the modes). For the results discussed below we use $N_m = 600$ which is indicated as dashed line in fig. 1, yet already $N_m = 300$ yields 95% of the quantitative accuracy.

4 Results

4.1 Softness field

In fig. 2a we show an exemplary snapshot of the softness field. One can clearly see the heterogeneous spatial distribution of soft regions across the simulation box. The black spheres are the first 100 hopping particles detected immediately after the measurement of the softness field, and some overlap is visible between hops and soft areas. The following sections are dedicated to the quantitative analysis of this correlation, yet we first focus on characteristics of the softness field itself. Fig. 2b shows the softness distribution in the entire polymer sample for different temperatures and ages. We find that the distributions feature a strong peak at small values and a rapid, yet slower than exponential decay. Our results show that the structural heterogeneity is remarkably similar for all studied systems.

In order for the softness field ϕ to represent the molecular structure in terms of "soft" and "hard" or stable and unstable regions, the lifetime of ϕ must match the structural lifetime. We measure the lifetime of the softness field via the decay of its autocorrelation function

$$C_a(t,t_{age}) = \left\langle \frac{\left[\phi(t_{age}) - \bar{\phi}(t_{age})\right]\left[\phi(t_{age}+t) - \bar{\phi}(t_{age}+t)\right]}{\sigma_{\phi(t_{age})}\sigma_{\phi(t_{age}+t)}} \right\rangle$$

Here, the average is over all particles, $\sigma_{\phi(t)}$ is the standard deviation of the softness field $\phi(t)$, and $\bar{\phi}(t)$ is its average. In

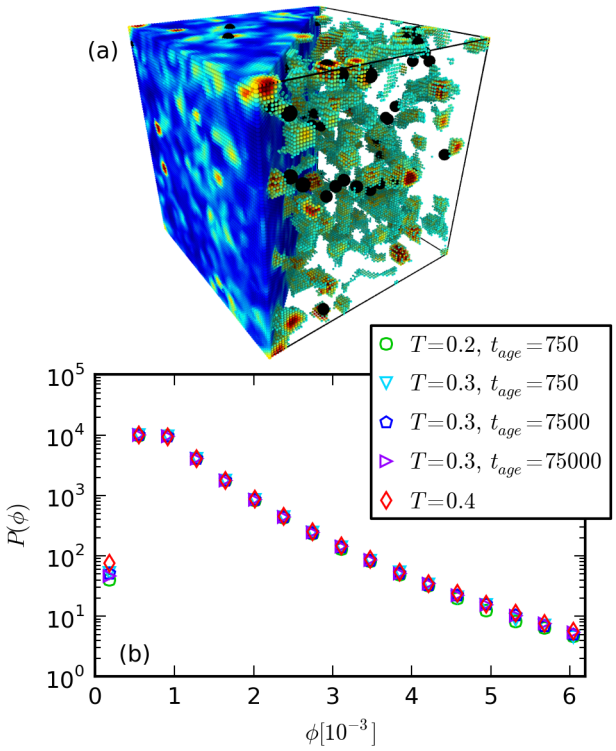

Fig. 2 (a) Snapshot of the softness field. The right side shows only the 10% softest regions and the solid black spheres (size equals particles) indicate the first 100 hopping particles detected after the measurement of the softness field. (b) Distribution of the softness field for three temperatures and three ages. Error bars are omitted and smaller than the symbols.

fig. 3 we show the autocorrelation for three temperatures (a-b) and three ages (c-d). All systems in the glass state exhibit an initial plateau in the ballistic regime, followed at intermediate times by a shoulder that becomes more pronounced at lower temperature and with increasing age. The final decay to zero has stretched exponential form and the autocorrelation reaches over many orders of magnitude in time. These characteristics are also found in the self-intermediate scattering function (ISF)

$$F_q^S(t,t_{age}) = \left\langle \exp\left[i\mathbf{q}\cdot(\mathbf{r}_j(t_{age}+t) - \mathbf{r}_j(t_{age}))\right]\right\rangle ,$$

which is the standard measure of structural lifetime[26]. Here, the average is over all particles and we use $\mathbf{q} = (0,0,2\pi)$. A value of $F_q^S(t,t_{age})$ close to zero means that most particles have moved further than their diameter away from their initial position. In fig. 3a,c the ISFs are indicated as dotted lines, and we observe two main differences when compared to C_a: First, the plateau and associated shoulder of the ISF are more pronounced and reach further in time. Second, the ISF decays to zero at later times than the autocorrelation. Before these

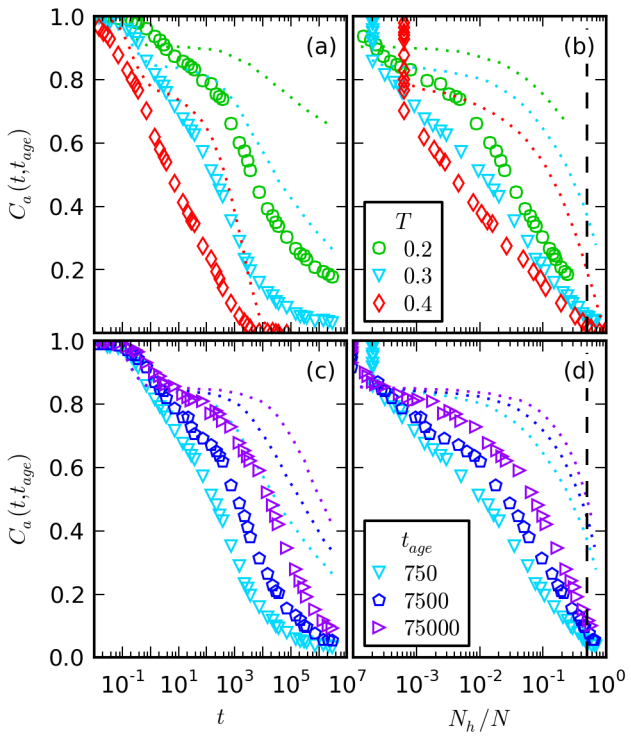

Fig. 3 Autocorrelation of the softness field for three temperatures (a-b) and three ages (c-d). Panel (a)[(c)] shows C_a as function of time, and the dotted lines indicate the ISF for the same temperatures [ages]. Panel (b)[(d)] shows C_a as function of number of hopped particles, with dotted lines again indicating the ISF and dashed lines mark when 50% of the system has hopped. Error bars are omitted and smaller than the symbols.

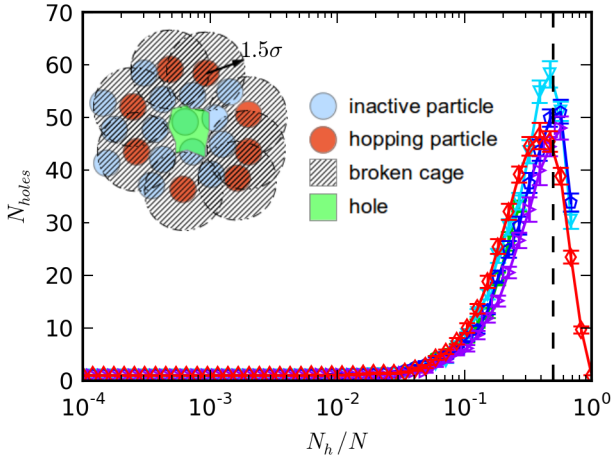

Fig. 4 Number of holes as a function of the fraction of hopped particles. The sketch illustrates the definition of a hole: a continuous volume (green) that is surrounded by the union of spheres that approximates the cages that hopping particles have escaped and are "broken". The dashed line indicates 50% of the system has undergone rearrangements, and the solid lines are guides to the eye. See fig. 2 for a legend.

differences are discussed in detail, we clarify the role of temperature and age on the autocorrelation of the softness field: Panel 3a shows that the decay-time becomes larger with decreasing temperature, as C_a shifts to the right. This is accompanied by the development of a shoulder at intermediate times, which is not present in the supercooled state ($T = 0.4$) but develops as the system becomes more glassy. This mimics the temperature dependence of the ISF, although a shoulder is already present in the supercooled state. In panel 3b we show how much of the system has undergone rearrangements as C_a decays by re-parametrizing time in terms of the fraction of particles that have hopped at least once. We observe that complete decorrelation of ϕ occurs for $T = 0.3, 0.4$ after $\gtrsim 50\%$ of particles have rearranged, and extrapolation suggests that this also holds true for $T = 0.2$. Panel 3c shows the autocorrelation for three ages at $T = 0.3$. We observe that an increase in age results in a shift of C_a towards larger times via lengthening of the shoulder. The ISFs are shown as dotted lines and one can see a similar shift with increasing age. In panel 3d we see that total decorrelation of ϕ again occurs when $\gtrsim 50\%$ of the system has undergone rearrangements, independent of the glass age.

A key difference between autocorrelation C_a and ISF is that the decorrelation of the softness field begins as soon as particles hop, whereas the ISF remains at a high value for much longer. However, this is not surprising, since the ISF can only change after a substantial part of the particles has moved. The structurally soft regions on the other hand may very well only require a few hops to transition into a more stable local configuration, which could explain the faster decay of C_a at intermediate times. It is also important to realize that the mean hop distance is of order half a particle diameter, while with a wavevector magnitude $q = 2\pi$ the ISF is sensitive to displacements of order one particle diameter. A particle therefore has to undergo multiple relaxation events to fully decorrelate the ISF, and in this sense the ISF decay provides an upper bound on the structural relaxation time.

Why does the softness field decorrelate after $\gtrsim 50\%$ of particles have hopped? To answer this question, we first note that a particle that hops by escaping its own local cage changes the local configuration of all the neighboring particles at the same time. To measure how much of the system has been affected by hops in this way, we place a sphere around each hopping particle with radius 1.5σ. This distance is the position of the first peak in the pair correlation function and the sphere therefore approximates the cage around each hopping particle. We then count the number of unconnected holes in the union of all

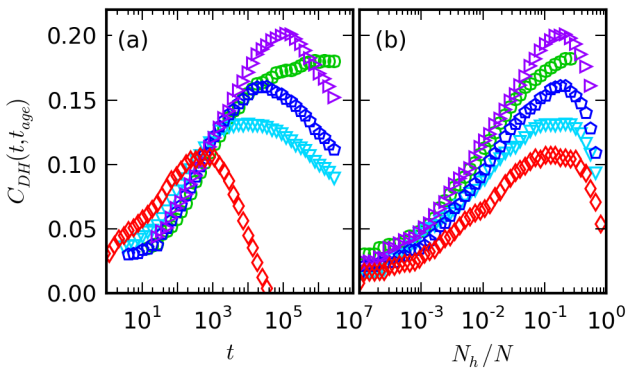

Fig. 5 Cross-correlation between softness field and cumulative map of hopped particles (a) as function of time and (b) as function of number of hopped particles. See fig. 2 for a legend, and error bars are omitted and smaller than the symbols.

spheres. The sketch in fig. 4 visualizes this: a hole is a continuous volume that is not part of any of the cages that are "broken" by the hopping particles. In the main panel of fig. 4 we show the number of holes as function of the fraction of hopped particles. When only a few particles have hopped, then there is only a single hole. As more particles hop, the spheres form clusters[22], interconnect and eventually percolate, leading to a subdivision into many holes. A maximum is reached, when the probability of splitting a hole in two by including an additional sphere is equal to the likelihood of destroying a hole. In other words, the maximum is reached, when the size of the holes is of the order of single cages. We find that this transition occurs when $\sim 50\%$ of the particles have hopped (indicated by the dashed line). At this time the total volume of the holes has dropped to $\sim 5\%$ of the system size. Therefore, the decorrelation of the softness field at $\gtrsim 50\%$ coincides with the change of the local configuration of nearly all particles.

4.2 Spatial correlation

In fig. 2a we show hops as black spheres together with the softness field, and one can see that hops appear at the center of soft regions as well as in the space between them. Before we analyze the overlap of individual hops with the softness field, we focus on the dynamical heterogeneity (DH) of the whole system. How well does a single measurement of a softness field reflect the distribution of regions with high/low rearrangement activity? We create a map of DH by accumulating hop events in a binary list h_i of all particles. The map changes as the time-window $[t_{age}, t_{age}+t]$ of included hops grows. The similarity of DH and the softness field is then quantified with the cross-correlation

$$C_{DH}(t,t_{age}) = \frac{\sum_{i=1}^{N}\left(h_i(t,t_{age})-\bar{h}(t,t_{age})\right)\left(\phi_i(t_{age})-\bar{\phi}(t_{age})\right)}{N\sigma_h\sigma_\phi}.$$

Here $\bar{h}$, $\bar{\phi}$ are averaged over all particles and σ_h, σ_ϕ are standard deviations. In fig. 5a we show the cross-correlation as a function of elapsed time after the ϕ measurement. A maximum is observed at times that grow with increasing age and decreasing temperature. The re-parametrization in terms of number of hopped particles in fig. 5b collapses the maxima at $\sim 20\%$ rearrangement of the system. The degree of agreement is given by the maximum value of the correlation, ranging from 0.11 for the supercooled system to 0.21 for the oldest glass at $T = 0.3$. The absolute value of the correlation is not very high, which can be expected from thermal systems. Simulations in the iso-configurational (IC) ensemble[2] reduce the impact of kinetics on the map of DH by averaging over many realizations of a single configuration with randomly assigned velocity distributions. We performed such an analysis on a single configuration of the system $T = 0.3, t_{age} = 75000$ and found a cross-correlation between the softness field and $\langle h_i \rangle_{IC}$ that is twice as strong at the peak. A systematic analysis using this technique, however, is beyond the scope of the present study.

The temperature and age dependence reveal the importance of the soft modes especially in the glass state. The increase of C_{DH} with age shows that the non-equilibrium state is important for the link between structure and dynamics. From the perspective of the potential energy landscape[27] (PEL): As the glass moves down the PEL towards more arrested, lower energy configurations, the soft modes increasingly dominate the dynamics of the glass. In the supercooled state we observe a lower correlation, indicating that higher temperature increasingly washes out the effect of structural heterogeneity defined by the soft modes. A lower temperature therefore yields a higher correlation. For the investigated temperature and age range both effects are of comparable magnitude and the largest correlation was found in the $T = 0.3$ glass after it was aged for two orders of magnitude longer than the $T = 0.2$ glass.

In fig. 6 we show two approaches that quantify the spatial correlation of relaxation events and softness field in greater detail: panel 6a shows the probability for a particle of given softness to undergo a hop at times immediately after the ϕ measurement, rescaled by the total hop probability

$$\Omega(\phi) = \frac{N_h(\phi)}{N(\phi)} \frac{\int d\phi N(\phi)}{\int d\phi N_h(\phi)}.$$

Here $N(\phi)$ indicates the number of particles with given softness and $N_h(\phi)$ is the subset of those particles that have hopped at least once. We observe a clear increase of the hop probability with increasing softness for all temperatures and ages. Starting from a value below one at very low ϕ (hard region), the probability monotonically rises to a saturation plateau of up to 7 times the average probability of relaxation events. The correlation is temperature dependent, being much more pronounced in the aging regime ($T = 0.2, 0.3$) than in the

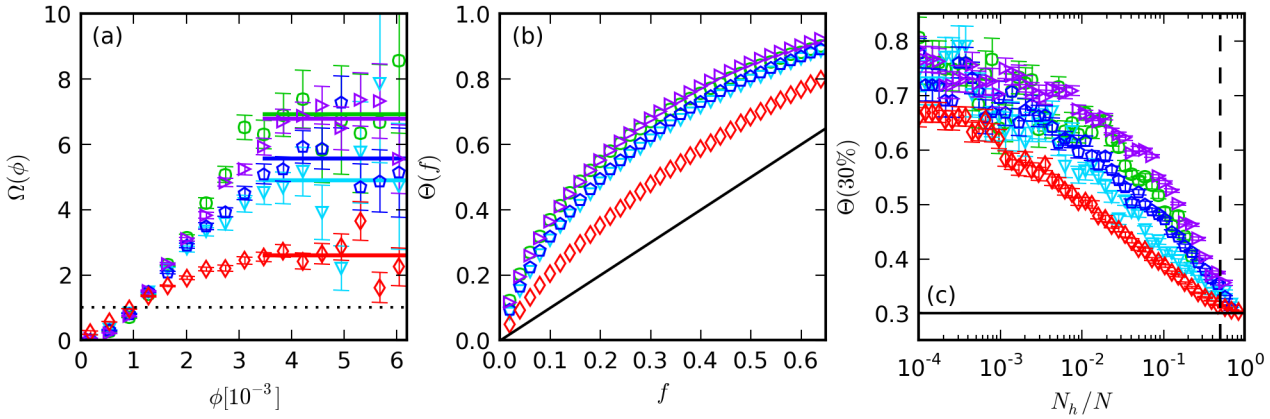

Fig. 6 (a) Probability of a particle to hop as function of its softness, rescaled by the average hop probability. The solid lines indicate the averaged saturation probability and the dotted line is a guide to the eye. Success rate of predicting hops to occur in the softest regions of the system Θ (b) as function of coverage fraction of the softest region f and (c) as function of time rescaled to the number of hopped particles at constant coverage fraction of $f = 30\%$. The solid lines in (b,c) indicate the success rate based on randomly chosen regions and the dashed line indicates 50% of the system has undergone rearrangements. To evaluate (a) and (b) the first 100 (1%) hopping particles after the softness field measurement were used. See fig. 2 for legend, and error bars are omitted when smaller than symbols.

supercooled system ($T = 0.4$), where the soft regions undergo rearrangements with three times the average probability. Furthermore, increased age yields a stronger correlation between soft modes and relaxation events.

We explore an alternative view on the spatial correlation by binarizing the softness field into a soft spot map, where the fraction of particles f with largest softness are assigned a softness of $\phi_i^{(b)} = 1$ and all other particles have a softness of zero. We then define the predictive success rate Θ of a softness field as the fraction of the first $N_h = 100$ hopping particles that are part of a soft spot, or

$$\Theta(f) = \frac{\sum_{i=1}^{N} \phi_i^{(b)} h_i}{N_h}$$

with $h_i = 1$ if particle i is one of the first N_h particles to hop after the measurement of the softness field, and $h_i = 0$ otherwise. Panel 6b shows the predictive success rate as function of the coverage fraction and a comparison with a randomly chosen subset of the system as soft spots is indicated by the solid line. Clearly, the softness field is a much better predictor, with the absolute difference being maximal at around 30% coverage fraction. Here, up to 70% of the first 100 hopping particles are predicted. Again, we find that systems at lower temperature show a stronger correlation and that increasing age also improves the predictive strength of the softness field. In panel 6c we show how the spatial correlation develops as function of time between the ϕ measurement and hops, i.e., shown is the predictive success rate for 30% coverage fraction. The time is rescaled in terms of the number of particles that have hopped at least once, identical to the rescaling in fig. 3 and fig. 5. The correlation is long-lived, decays logarithmically and decorrelates only when $\gtrsim 50\%$ of the system has undergone structural relaxation events.

4.3 Directional correlation

The direction of the softness field, which is the average direction of the soft modes, contains information about the *dynamics* of the relaxation events. More precisely, the direction of the hops align with the direction of the softness field in soft regions. We quantify this correlation via the second Legendre polynomial

$$C_d = \langle \frac{3}{2} \left(\hat{\mathbf{d}} \cdot \mathbf{e}_\phi \right)^2 - \frac{1}{2} \rangle \,,$$

where $\hat{\mathbf{d}} = (\mathbf{r}_f - \mathbf{r}_i)/|\mathbf{r}_f - \mathbf{r}_i|$ is the unit vector between final and initial position of a hopping particle, and $\mathbf{e}_\phi$ is the direction of the softness field for the same particle (see section 2.1). The average is taken over hopping particles. A value of $C_d = 1$ means full alignment of hop and softness field direction, while $C_d = 0$ indicates that a random orientation with respect to each other. In fig. 7a we show the correlation immediately after the measurement of ϕ as function of softness. The alignment grows with increasing ϕ for all temperatures and ages until a saturation plateau is reached. Similar to the spatial correlation discussed above, increased temperature weakens the link between the soft modes and the hops. The saturation value reaches from 0.4 for the supercooled system to 0.8 for the glass at $T = 0.2$, indicating that hops are nearly perfectly aligned with the softness field direction at low temperatures. The effect of aging, however, seems to be negligible for the

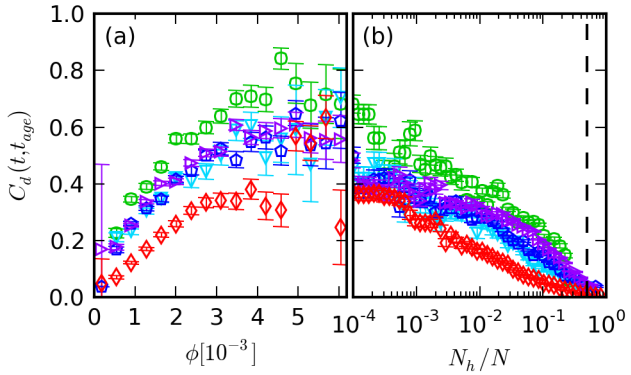

Fig. 7 Directional correlation between softness field and hops (a) as function of softness and (b) as function of time rescaled to the number of hopped particles. The dashed line indicates 50% of the system has undergone rearrangements and the hop direction is measured as the vector between initial and final position of the particle. To evaluate (a) the first 100 (1%) hopping particles after the softness field measurement were used. See fig. 2 for a legend.

strength of the directional correlation. This behavior is qualitatively different from the age-dependent spatial correlation, which grows with increasing age. Our finding implies that the direction of molecular relaxation events is independent of the position on the PEL, because the later is changed during aging. In other words, the non-equilibrium nature of the glass has no direct impact on the alignment of soft modes and hops. Temperature on the other hand acts as noise and reduces the degree of alignment.

In panel 7b we show the mean directional correlation as function of number of hopped particles since the measurement of ϕ. We observe a slow logarithmic decay of the correlation that vanishes only after $\gtrsim 50\%$ of the system has hopped at least once, for all temperatures and ages. A close inspection reveals that at increased age, the decay curve develops a small shoulder around $1\% - 10\%$ hopped particles. This behavior does not indicate a direct age-dependence, but rather is a consequence of the longevity of the softness field itself. The autocorrelation data discussed in section 4.1 shows how aging leads to an increased stability of ϕ in the range of $< 50\%$ hopped particles. The decay curves for the directional correlation reflect this longevity, showing that the softness field direction has predictive strength over the direction of hops until the local configuration of nearly all particles has changed.

5 Conclusions

We quantitatively studied the correlation between soft modes and segmental relaxation events in a simple bead-spring polymer glass model. The system was simulated in the quiescent state at two temperatures below T_g in the aging regime and one above T_g in the supercooled regime. Furthermore, one system in the aging regime was analyzed at three ages. The structural relaxation events were identified as hops in the particle trajectories using a previously introduced algorithm[22]. We quantified the participation of particles in soft modes in terms of a *softness field* ϕ, which we constructed from a superposition of low energy vibrational eigenmodes[7]. It is closely related to the binary soft spot approach[13], but here the sole adjustable parameter is the number of included modes.

For all temperatures and ages the softness field was found to be heterogeneous, with small regions of large softness. We showed that a strong correlation exists between the softness of a particle and its likelihood of undergoing a structural relaxation event. Starting from a much decreased probability at small ϕ, we found that with growing softness the hop probability increases to up to 7 times the average value. The spatial correlation is stronger at lower temperature and also grows with increasing age. We showed that a binary soft spot map based on ϕ with 30% coverage fraction predicts up to 75% of the hops immediately following the ϕ-measurement. The predictive strength was found to decrease slowly with increasing time separation between ϕ-measurement and hops. The correlation vanishes for all temperatures and ages only after $\gtrsim 50\%$ of the polymer glass has undergone rearrangements, which coincides with the decay of the softness autocorrelation function. The softness field and the binarized soft spots that can be derived from it are therefore long lived features that capture the heterogeneity of the amorphous structure.

In addition to the *spatial* correlation of hops to soft regions in the glass, we were able to show that the soft modes also correlate to the dynamics of relaxation events. The *direction* of hops, measured as displacement vector between initial and final position of the particle, are correlated to the soft mode directions. We find an increasing alignment with increasing softness that reaches values of 70% for the lowest temperature glass. The correlation is again stronger at lower temperature, yet it appears to be independent of the glass age. An older soft spot will attract more hops and hence has a larger spatial correlation than a younger soft spot, but hops actually occuring on a soft spot follow the soft directions independent of age.

Our findings are in good quantitative agreement with a recent study[14] on a sheared 2D binary mixture at finite temperature. This study found rearrangements to be 2-3 times more probable at soft spots than at random locations. A detailed analysis of the individual soft spot dynamics showed that they are robust structures that reach lifetimes of up to the bulk structural relaxation time scale, which agrees with our analysis of the ϕ autocorrelation function. In the driven systems, there is a closer relationship between self-intermediate scattering function and soft spot decay as in the present quiescent case. This may be due to extremely long local persistence times which here are not bound by an imposed external

drive. Both spatial and directional correlations were furthermore identified in a recent study[28] that investigated the role of soft modes at the crossover between ordered to disordered systems. Soft modes were observed to predict the direction and location of rearrangements in a hierarchy of systems: from a crystal with a single dislocation, to a polycrystal and a binary glass in 2D.

A growing body of research is indicating that soft modes are indeed linking irreversible rearrangements, plasticity and microscopic structure in amorphous solids. Evidence has been found in a diverse set of model systems mostly in 2D, but this study adds quantitative evidence in 3D: From binary supercooled liquids in the quiescent state[7,8,29], sheared binary glasses at zero temperature[11,13,15] and finite temperature[14], to polycrystals[28], lattice models[10] and the present quiescent polymer glasses in the supercooled and aging regime. Various measures for rearrangements have been used, ranging from the change of nearest neighbors[7], to maxima in the non-affine displacement field[14], and here hops in individual particle trajectories. Moreover, soft modes were quantified in different ways: correlations to rearrangements were identified w.r.t. individual modes[11], the binary soft spot field[13] and the here used superposition of participation fractions[7]. Despite these variations in simulated models and analysis, the robustness of the correlation suggests, that soft spots should play a prominent role in theories of plasticity for amorphous solids in general, and the practically important case of polymer glasses in particular.

A second approach to understand the cause of dynamical heterogeneity in amorphous solids has developed around the discovery of heterogeneously distributed local elastic moduli[30–33]. Regions of small shear moduli were found to be prone to plastic rearrangements, whereas areas with high moduli tend to be more structurally stable. Both approaches are closely related as they are harmonic theories and some work has been done to understand the link between them[18]. It would be interesting to further explore the relationship between soft modes and local elastic moduli, and directly analyze both spatial distributions. Do soft spots indeed have a small shear modulus, and are the decay timescales of the heterogeneous distributions related? It is furthermore important to explore the reliability of the soft mode picture in mechanically deformed polymer glasses under different deformation protocols, which is a scenario of large practical importance.

Acknowledgments

We thank A. J. Liu and S. S. Schoenholz for stimulating discussions. This work has been supported by the Natural Science and Engineering Research Council of Canada (NSERC). Computing resources were provided by WestGrid/Compute Canada.

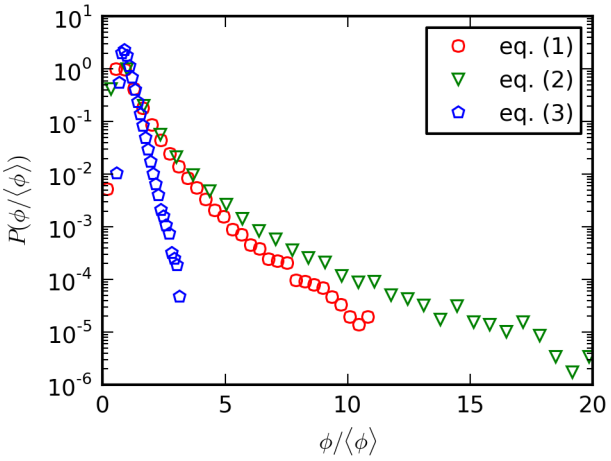

Fig. 8 Distribution of softness in the system $T = 0.3$, $t_{age} = 750$ for three definitions of the softness field. The softness is rescaled in terms of the mean softness to allow an easier comparison.

6 Appendix

The definition of a field that quantifies the participation of particles in soft modes is not well understood. The superposition of participation fractions used here and in several other studies[7,8,15] essentially measures the average potential energy of the particles. To see this, note that the participation fractions distribute the total potential energy $\langle U_j \rangle$ of mode j over particles i so that $\langle U_j^{(i)} \rangle = \langle U_j \rangle |\mathbf{e}_j^{(i)}|^2$, and $\langle ... \rangle$ denotes a thermal rather than disorder average. The softness field defined in eq. (1) is therefore proportional to the *mean potential energy* of particle i in the N_m lowest energy modes, assuming equipartition of the mode energies. However, as mentioned in section 2, participation in lower energy modes should be more important than in higher energy modes, since less energy is needed to displace a particle from its inherent structure position. In this view, the softness of a particle becomes proportional to its *mean squared vibrational amplitude* $\langle x_j^{(i)2} \rangle = 2\langle U_j^{(i)} \rangle / m\omega_j^2$, and the softness field becomes

$$\phi_i = \frac{1}{N_m} \sum_{j=1}^{N_m} \frac{|\mathbf{e}_j^{(i)}|^2}{m\omega_j^2} \,. \tag{2}$$

Finally, one may ask why the mean squared vibrational amplitude should be considered rather than the *mean absolute* or rms amplitude. This leads to a third alternative for the softness field

$$\phi_i = \frac{1}{N_m} \sum_{j=1}^{N_m} \frac{|\mathbf{e}_j^{(i)}|}{\sqrt{m\omega_j^2}} \,. \tag{3}$$

In fig. 8 we compare the distributions of softness resulting from these three alternative definitions. We find that the

weighting w.r.t. mode energy given in eq. (2) stretches the distribution obtained from eq. (1) without changing it qualitatively. Using the average displacements as measure on the other hand yields a qualitatively different, purely exponential distribution of softness. This exponential form reminds of the self-part of the van Hove function, which measures the distribution of particle displacements as function of elapsed time. A key characteristic of glasses is the non-Gaussian, exponential tail found in the van Hove function, and the softness field based on eq. (3) seems to hold a fingerprint of this feature of glassy dynamics. We also compared the spatial and directional correlation of the softness based on eqns. (1-3) to hops (not shown). The results are remarkably insensitive qualitatively as well as quantitatively, with eq. (3) yielding a slightly better spatial correlation. We choose to report our results in terms of eq. (1) for ease of comparison with previous studies in other systems.

References

1 M. D. Ediger, *Annu. Rev. Phys. Chem.*, 2000, **51**, 99–128.
2 A. Widmer-Cooper, P. Harrowell and H. Fynewever, *Phys. Rev. Lett.*, 2004, **93**, 135701.
3 L. Berthier and R. L. Jack, *Phys. Rev. E*, 2007, **76**, 041509.
4 B. B. Laird and H. R. Schober, *Phys. Rev. Lett.*, 1991, **66**, 636–639.
5 H. R. Schober and C. Oligschleger, *Phys. Rev. B*, 1996, **53**, 11469–11480.
6 U. Buchenau, C. Pecharroman, R. Zorn and B. Frick, *Phys. Rev. Lett.*, 1996, **77**, 659–662.
7 A. Widmer-Cooper, H. Perry, P. Harrowell and D. R. Reichman, *Nat Phys*, 2008, **4**, 711–715.
8 A. Widmer-Cooper, H. Perry, P. Harrowell and D. R. Reichman, *The Journal of Chemical Physics*, 2009, **131**, 194508.
9 C. Brito and M. Wyart, *J. Stat. Mech.*, 2007, **2007**, L08003.
10 D. J. Ashton and J. P. Garrahan, *The European Physical Journal E*, 2009, **30**, 303–307.
11 A. Tanguy, B. Mantisi and M. Tsamados, *EPL*, 2010, **90**, 16004.
12 K. Chen, M. L. Manning, P. J. Yunker, W. G. Ellenbroek, Z. Zhang, A. J. Liu and A. G. Yodh, *Phys. Rev. Lett.*, 2011, **107**, 108301.
13 M. L. Manning and A. J. Liu, *Phys. Rev. Lett.*, 2011, **107**, 108302.
14 S. S. Schoenholz, A. J. Liu, R. A. Riggleman and J. Rottler, *arXiv:1404.1403 [cond-mat]*, 2014.
15 M. Mosayebi, P. Ilg, A. Widmer-Cooper and E. Del Gado, *Phys. Rev. Lett.*, 2014, **112**, 105503.
16 N. Xu, M. Wyart, A. J. Liu and S. R. Nagel, *Phys. Rev. Lett.*, 2007, **98**, 175502.
17 H. Shintani and H. Tanaka, *Nat Mater*, 2008, **7**, 870–877.
18 P. M. Derlet, R. Maaß and J. F. Löffler, *Eur. Phys. J. B*, 2012, **85**, 1–20.
19 K. Kremer and G. S. Grest, *J. Chem. Phys.*, 1990, **92**, 5057.
20 C. Bennemann, W. Paul, K. Binder and B. Dünweg, *Phys. Rev. E*, 1998, **57**, 843–851.
21 M. P. Allen and D. J. Tildesley, *Computer Simulation of Liquids*, Oxford University Press, 1989.
22 A. Smessaert and J. Rottler, *Phys. Rev. E*, 2013, **88**, 022314.
23 S. Plimpton, *J. Comput. Phys.*, 1995, **117**, 1–19.
24 E. Bitzek, P. Koskinen, F. Gähler, M. Moseler and P. Gumbsch, *Phys. Rev. Lett.*, 2006, **97**, 170201.
25 D. Sorensen, R. Lehoucq, C. Yang and K. Maschhoff, *ARPACK can be found at http://www.caam.rice.edu/software/ARPACK/*.
26 J.-P. Hansen and I. R. McDonald, *Theory of Simple Liquids*, Academic Press, 2006.
27 A. Heuer, *Journal of Physics: Condensed Matter*, 2008, **20**, 373101.
28 J. Rottler, S. S. Schoenholz and A. J. Liu, *Phys. Rev. E*, 2014, **89**, 042304.
29 G. M. Hocky and D. R. Reichman, *The Journal of Chemical Physics*, 2013, **138**, 12A537.
30 K. Yoshimoto, T. S. Jain, K. V. Workum, P. F. Nealey and J. J. de Pablo, *Phys. Rev. Lett.*, 2004, **93**, 175501.
31 G. J. Papakonstantopoulos, R. A. Riggleman, J.-L. Barrat and J. J. de Pablo, *Phys. Rev. E*, 2008, **77**, 041502.
32 M. Tsamados, A. Tanguy, C. Goldenberg and J.-L. Barrat, *Phys. Rev. E*, 2009, **80**, 026112.
33 H. Mizuno, S. Mossa and J.-L. Barrat, *Phys. Rev. E*, 2013, **87**, 042306.